IOP Publishing Measurement Science and Technology

Meas. Sci. Technol. **19** (2008) 075202 (9pp) doi:10.1088/0957-0233/19/7/075202

Foot mounted inertial system for pedestrian navigation

S Godha and G Lachapelle

Position Location and Navigation Group, Department of Geomatics Engineering, The University of Calgary, 2500 University Drive, Calgary, AB, T2N 1N4, Canada

E-mail: saurabhgodha@gmail.com

Received 10 September 2007, in final form 19 March 2008
Published 29 May 2008
Online at stacks.iop.org/MST/19/075202

Abstract

This paper discusses algorithmic concepts, design and testing of a system based on a low-cost MEMS-based inertial measurement unit (IMU) and high-sensitivity global positioning system (HSGPS) receivers for seamless personal navigation in a GPS signal degraded environment. The system developed here is mounted on a pedestrian shoe/foot and uses measurements based on the dynamics experienced by the inertial sensors on the user's foot. The IMU measurements are processed through a conventional inertial navigation system (INS) algorithm and are then integrated with HSGPS receiver measurements and dynamics derived constraint measurements using a tightly coupled integration strategy. The ability of INS to bridge the navigation solution is evaluated through field tests conducted indoors and in severely signal degraded forest environments. The specific focus is on evaluating system performance under challenging GPS conditions.

Keywords: GPS, INS, MEMS, pedestrian navigation, PDR

(Some figures in this article are in colour only in the electronic version)

Introduction

Integration of Global Positioning System (GPS) and low-cost MEMS-based inertial measurement units (IMU) has recently gained much attention for positioning in consumer-based navigation applications, e.g. Kealy *et al* (2001), Cao *et al* (2002), Lachapelle *et al* (2003), Mezentsev (2005) and Godha (2006). The majority of these applications are linked to land vehicle navigation systems (LVNS) that provide route guidance to users when traveling in a vehicle. However, after stepping out of the vehicle, in order to reach a particular destination, the user typically has to walk an appreciable distance as a pedestrian. Thus, a system that is able to provide additional navigation assistance for the last segment that the user has to walk to reach the destination point is of great interest. Such systems are called pedestrian navigation systems (PNS). There is a significant demand for such devices for different safety specific and commercial applications such as military, fire-fighting and location-based services (LBS). One of the most important components required to get a location of a person is the positioning technology. Thus the aim of this research is to develop and test algorithmic concepts for positioning in a pedestrian navigation system.

The issue of positioning might appear fairly easy to resolve given technologies such as global positioning system (GPS), which has now been used for over 20 years. However, a closer look into this technology reveals its limitations from a personal positioning perspective. A PNS typically has to operate in areas where GPS signals are either blocked or severely degraded (such as urban areas, forest areas and indoors), which limits its capability to maintain continuity of positioning. Having said that, technological advancements have now made it feasible to track GPS signals under degraded signal environments, using long pre-detection integration (PIT) times and assistance from external sources, i.e. assisted GPS (AGPS) (Karunanayake *et al* 2004). However, the reliability and accuracy of such techniques is questionable (e.g. MacGougan (2003), Lachapelle (2006)). Therefore, to enable continuity in personal navigation and to ensure navigation when the subject moves indoors, integration of GPS with other complementary self-contained navigation sensors, such as inertial measurement unit (IMU), is necessary.

In general, for positioning in a PNS, the IMU measurements are used in a pedestrian dead-reckoning (PDR) algorithm for computing the positions, e.g. Ladetto (2000), Stirling *et al* (2003), and Mezentsev *et al* (2005). In a PDR algorithm, the positions are computed by detecting the user's step and propagating the estimated step-length in the direction of motion. This relieves the PDR algorithm from the inherent integration (over time) process involved in inertial navigation system (INS) algorithm, which causes a large error accumulation (in the absence of aiding source) because of integration of sensor errors. However, as discussed in Godha *et al* (2006), the choice of algorithm often depends on the sensor positioning on the user's body. The specific focus of this paper is on the use of foot mounted inertial sensors (see figure 1). For such sensor positioning it is generally preferable to use an INS algorithm. The reason for this is two-fold. Firstly, when the sensor is placed on the foot, the dynamics of the foot enable the use of frequent zero velocity updates (ZUPTs), which eliminates the problem of error accumulation over time and thus significantly extends the ability of INS to maintain accuracies within desired bounds for longer periods (Godha *et al* 2006). Secondly, an INS provides a six degree-of-freedom (DOF) navigation solution which can efficiently track different modes of walking, for instance walking forward, backward, side-stepping or any other non-standard pedestrian motion, without any need for extra modeling (extra modeling is required for the case of a PDR algorithm).

Foot mounted systems have been investigated before, for instance, Stirling *et al* (2003) used a sensor system comprised of an array of accelerometers and a magneto-resistive sensor system with a PDR algorithm for computation of navigation solution. Cavallo *et al* (2005) used a foot-mounted inertial sensor system, comprised of two accelerometers and a gyro and achieved remarkable accuracies.

The MEMS IMU used herein is the Crista IMU from Cloud Cap Technology. The Crista IMU is very small in size and weighs only 37 gm (Crista Interface/Operation Document 2004). The GPS receiver being used in this study is the SiRF Star III HSGPS receiver. The sensitivity level of the SiRF Star III is down to −189 dBW. This allows the receiver to track a high number of satellites and provide more measurements; however, it also makes the receiver more prone to tracking cross-correlation and echo-only signals (McGougan 2003). Thus, efficient reliability checking of GPS measurements is important, in order to prevent the use of faulty measurements in the integration filter.

The specific emphasis of this paper is on the performance evaluation of ZUPTs aided GPS/INS system in challenging GPS environments. Field tests were conducted under two different environments: (1) indoors—to assess the system performance under complete GPS unavailability; and (2) signal degraded forest environment—to assess the system performance under frequent complete/partial GPS outages and to assess the impact of HSGPS receiver noise and multipath effects on the integrated navigation solution. The results are presented in terms of position accuracy, navigation solution continuity and availability using different methods.

Figure 1. Foot mounted inertial sensor.

System design

The IMU measurements are processed through an INS algorithm which is a fairly well-understood algorithm and consists of a set of mechanization equations that converts the raw IMU measurements into useful navigation information. The mechanization for this study is implemented in the earth-centered earth-fixed (ECEF) frame. For details on INS mechanization, please refer to Savage (2000), Farrell and Barth (2001), and Godha (2006).

The INS computed navigation solution from the IMU raw measurements consists of errors driven by the sensor measurement errors. In order to correct for these errors, an INS filter (Kalman filter) is set up, which uses the standard 15-state INS *phi-angle* error model (Savage 2000, Salychev 1998, Scherzinger 2004) and estimates the errors using the raw GPS measurements, as an update source, in a differential mode. This integration mode, where integration is performed at the measurement level, is called a tightly coupled integration strategy. When GPS is not available, the INS operates in a prediction mode, and the output of the INS mechanization forms the final navigation solution. The performance during this period depends on the quality of the inertial sensor and how well its measurement errors are compensated (e.g. sensor biases and scale factors). The error compensations, especially for MEMS sensors, in general are not accurate given the large random bias variations and high sensor noise, which makes it difficult to correctly model using stochastic processes. This ultimately results in accumulation of errors in the absence of aiding source causing divergence in the navigation solution.

In the system designed here the inertial sensor is placed on a foot. The fact that the foot comes to rest (i.e. velocity ∼0) every time it strikes the ground (figure 2) can effectively be used to prevent INS error accumulation. A foot typically remains in the stance phase during about 25% of the gait cycle (Chai 2004), and a gait cycle for an adult walking at normal speed typically lasts for 1.2 to 1.3 s. This means that the foot comes to rest almost every second and velocities can be set as zero. Velocities are actually not set directly to zero; instead zero velocity update (ZUPTs) measurements are used to exploit the correlation between velocity errors and various inertial sensor and attitude errors. The frequent use of ZUPTs reduces the time window of INS predictions to less than a second, ultimately leading to significantly improved navigation performance.

In order to use ZUPTs in the integrated system, it is necessary to detect automatically when the user's foot is at rest. This is basically a pattern recognition problem and can be

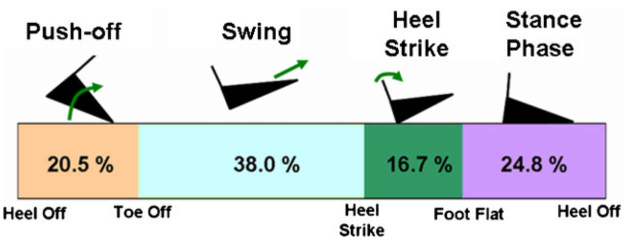

Figure 2. Gait cycle (adapted from Chai (2004)).

accomplished by analyzing the signature of the accelerometer signals. When the sensor is placed on a foot, the accelerometer signature demonstrates specific repeatability corresponding to each phase of the gait cycle, as shown in figure 3. Clearly the pattern being sought is when the magnitude of the 3D acceleration sensed by the accelerometer is close to the earth's gravity. For automatic detection of this phase, a two-step algorithm is used. The first step is based on the magnitude of the accelerometer signal and uses the moving acceleration variance over 'n' samples. The value of n is taken as 3 (the IMU sampling rate is set to 100 Hz), which was obtained empirically through signal analysis. If the acceleration magnitude and computed moving variance ($\sigma_{k,k-3}$) are within the predefined threshold value ($\sigma_{\text{threshold}}$), then a stance phase can be declared. The second condition checks for the minimum time separation between the current time (time for ZUPT, t_k) and the 'start time (t_s)' of the last step. Steps are also detected by computing the moving variance over 'n' samples; however, the sample size here is taken as 30, which is determined empirically, and is a function of IMU sampling rate (for further details please refer to Godha *et al* (2006)). Thus, the stance phase is declared when the following two conditions are satisfied:

$$\sigma_{k,k-3} < \sigma_{\text{threshold}} \quad \text{and} \quad t_k - t_s > \Delta t \qquad (1)$$

Figure 4 shows the accelerometer signal and variance pattern and the detected ZUPTs using this algorithm. The integration strategy is summarized in figure 5.

INS error observability through ZUPTs

To understand the INS error observability through ZUPT measurements, consider the velocity-error dynamics equation in the local level frame (LLF) (El-Sheimy 2004):

$$\begin{bmatrix} \delta\dot{v}^e \\ \delta\dot{v}^n \\ \delta\dot{v}^u \end{bmatrix} = \begin{bmatrix} 0 & f^u & -f^n \\ -f^u & 0 & -f^e \\ f^n & -f^e & 0 \end{bmatrix} \begin{bmatrix} \delta\eta \\ \delta\xi \\ \delta\psi \end{bmatrix} + \begin{bmatrix} \delta f^e \\ \delta f^n \\ \delta f^u \end{bmatrix} \qquad (2)$$

where the dot represents the time derivative, δv^i denotes the velocity errors in LLF, f is the specific force in LLF, $\delta\eta$ is the pitch error, $\delta\xi$ is the roll errors, $\delta\psi$ is the heading errors and δf^i is the accelerometer sensor errors in LLF.

It can be seen from equation (2) that the north- and east-velocity errors are correlated with the pitch and roll errors through the specific force in the up direction, which is typically close to average gravity on the earth's surface (9.8 m s^{-2}). Consequently, a strong coupling exists between the tilt estimation and the horizontal velocities. This means that accurate estimation of velocity-error states through ZUPTs not only improves the accuracy of velocity estimation, but also the accuracy of computed roll and pitch angles (and

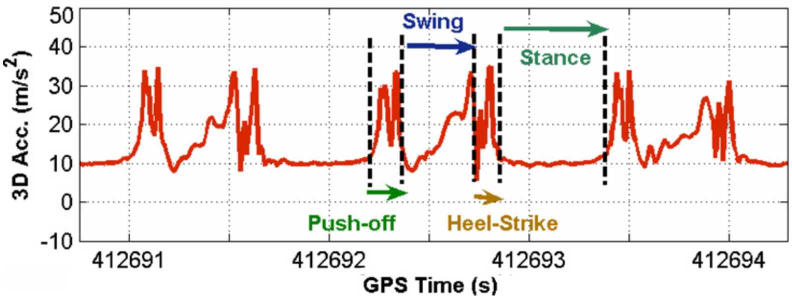

Figure 3. Accelerometer signal and gait phases.

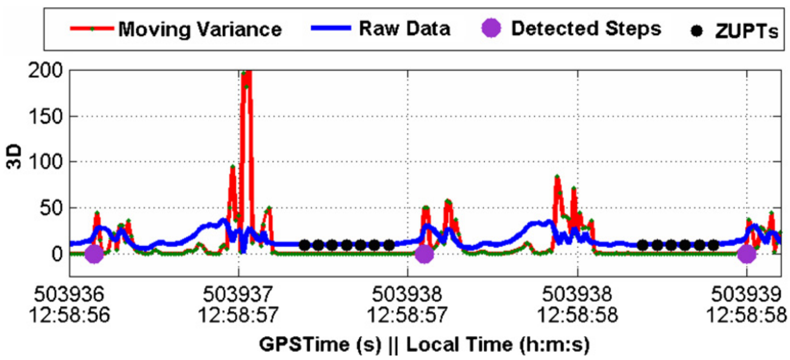

Figure 4. Accelerometer moving variance and detected steps and ZUPTs.

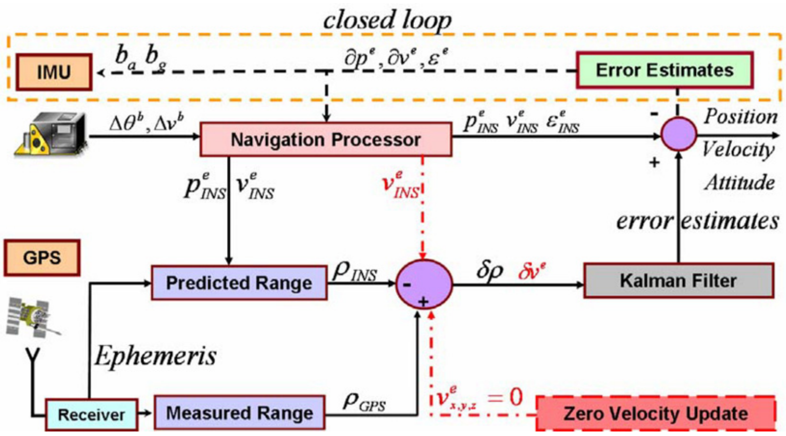

Figure 5. Tightly coupled integration strategy with ZUPTs.

the subsequent *y* and *x* gyro biases). However, the errors in heading are related through the north and east specific forces, which theoretically should be zero when ZUPTs are used. This makes heading errors (and the subsequent *z* gyro bias) poorly observable through ZUPT measurements. This means that the heading errors in the system can only be computed when GPS is available, and thus becomes a primary error-contributing factor in the integrated system when GPS is not available.

Software implementation

The GPS/INS (/PDR) integration software used herein is described by Godha (2006) and Godha *et al* (2006), and was developed using C++. The software has a GPS processing component, an INS processing component, a PDR processing component, GPS/INS and GPS/PDR integration component, error compensation component and a backward smoothing component.

GPS processing is done in single differential mode using L1 C/A code (and Doppler) measurements. The GPS/INS integration filter state model is flexible in nature, where different sensor error characterization states can be switched on or off depending on the quality of the IMU being used and the application being considered. The PDR component implements algorithm to detect steps and estimate step-lengths for the cases when the sensor is placed on a foot and on a shoulder. The integrated navigation module integrates both INS and PDR with GPS using a loosely and a tightly coupled integration scheme. With minimal adjustments, the software can be used for either vehicular or pedestrian navigation applications (for shoulder and shoe mounted sensors), where it can use application-specific dynamics-derived constraints to keep the system errors bounded. Figure 6 shows the software implementation flow for operation in vehicle and walking mode. The software runs different components at different rates, depending on the sensors data rates. In this study, the INS mechanization (i.e. computation of INS positions, velocities and attitude) is run at 20 Hz. It is noted that for a PNS device such high navigation output rates are neither required nor desired, in order to minimize the computational load in the portable device when operating in real time. However, since the dynamics experienced by the IMU on the user's feet are quite high (angular rates typically reach up to 400° s^{-1} at normal walking speeds), the mechanization is run at high frequency to avoid any errors in the computation of attitude angles due to lower resolution. The mechanization loop is followed by update either using dynamics-derived constraints such as ZUPTs and/or GPS depending on the mode of operation and the availability of the measurements. For the results shown here, only the GPS/INS aspect of the software was used and the processing is carried out using a tightly coupled integration scheme.

Indoor test

To verify the feasibility of using the system for indoor applications, several tests were performed on a single floor inside the CCIT building at the University of Calgary[1], with the INS sensor placed on a foot. For these tests, no GPS was used, i.e. the navigation solution is based on INS/ZUPTs. Figure 7 shows the solution computed by the system. The user started in at point (0, 0), walked through an entrance door, toward another location, then returned through the same path, and completed three loops in the floor corridors. The test ended at the same location as the start point. The total duration of the test was 3.5 min, and the total distance traveled was 270 m.

As can be noted from the figure, the INS predicted the navigation solution quite well given that the only source of updates was ZUPTs. The derived trajectory seems slightly skewed relative to the reference trajectory, especially during the 2nd and 3rd loops in the 3rd floor corridor. The primary cause for this behavior is the divergence in the heading solution. Since heading is not observable with ZUPTs, its accumulated error ultimately caused a separation of 3.3 m (1.2% of the total distance traveled) between the end

[1] References pertaining to the University of Calgary can be downloaded from the following links: http://www.geomatics.ucalgary.ca/research/publications/GradTheses.html and http://plan.geomatics.ucalgary.ca/publications.php

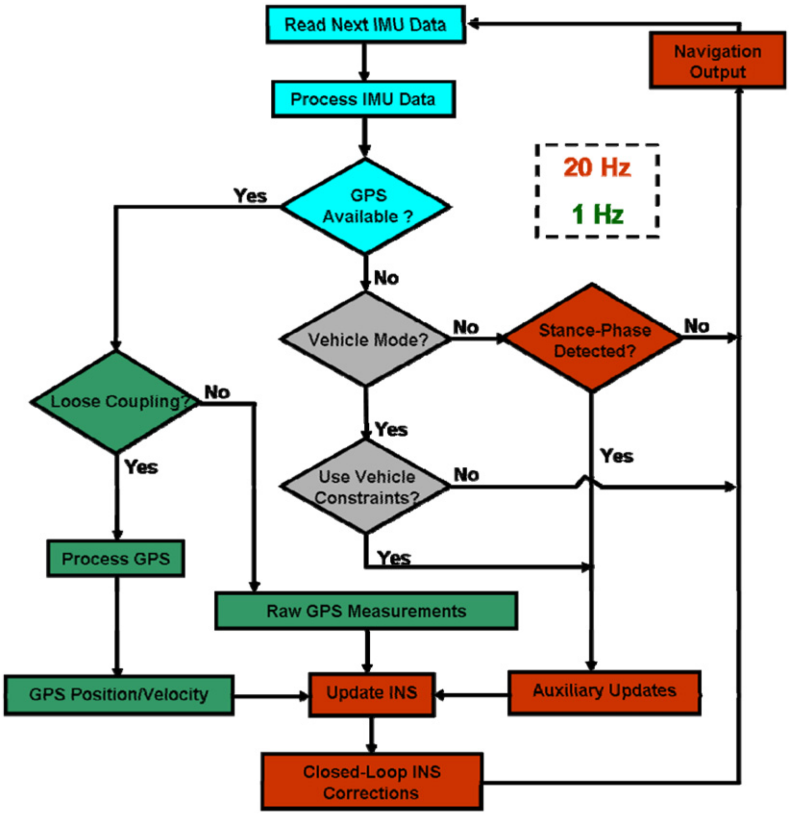

Figure 6. Software implementation (GPS/INS aspect).

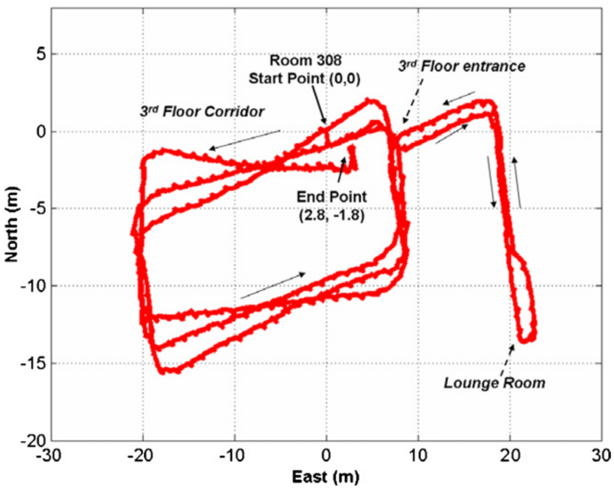

Figure 7. Indoor walking: CCIT 3rd floor.

point and the start point of the trajectory. Thus for using the system indoors, heading updates from external sources such as a magnetometer are preferable, provided magnetic disturbances can be avoided.

Outdoor test

This test was conducted in a Calgary city park. This area was chosen since it features dense foliage environments, with lines of trees on both sides of the walkway (figure 8), which caused significant signal blockage and attenuation.

Figure 8. Test area.

The inertial data were collected using a tactical grade HG1700 IMU and the Crista IMU. The Crista IMU was mounted on the foot while HG1700 IMU was placed in the backpack. The solution computed with the HG1700 unit was used as a reference to assess the performance of the Crista IMU. Both sensors collected data at a 100 Hz rate. The GPS data were logged using three different GPS receivers, namely a NovAtel OEM4 receiver, a SiRF Star III HSGPS receiver and a u-blox HSGPS receiver. All three receivers

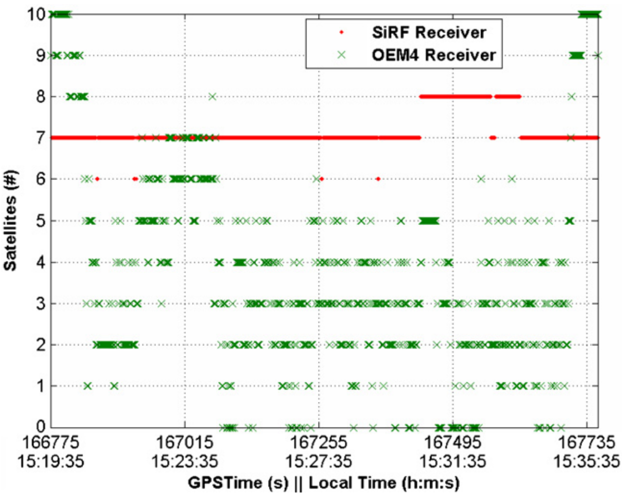

Figure 9. Satellite visibility with OEM4 and SiRF receivers.

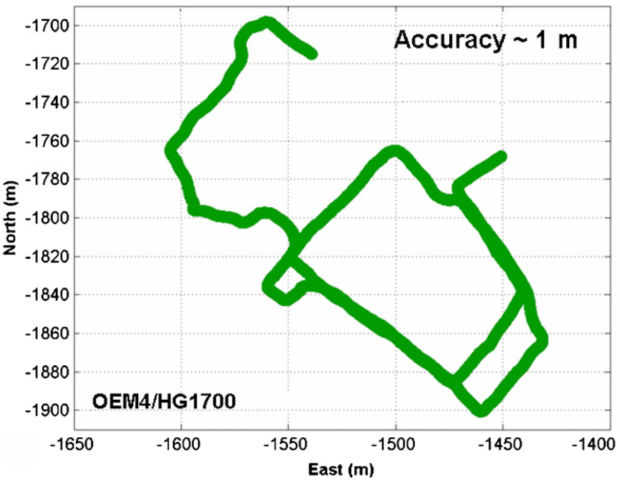

Figure 10. Reference trajectory.

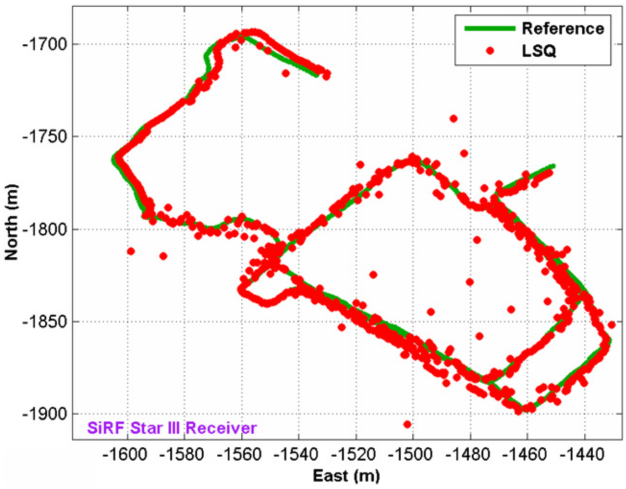

Figure 11. Epoch-by-epoch GPS only solution—SiRF Star III receiver.

were connected to one GPS antenna via a signal splitter, which was then mounted on the user's backpack. The OEM4 receiver was integrated with the HG1700 unit to generate the reference solution using the software's smoothing component. The SiRF Star III receiver data were used to generate the performance testing results of the designed system.

The duration of the test run was 18 min, and the user took about 660 steps and walked a total distance of about 900 m. The satellite visibility with the standard OEM4 receiver and the high sensitivity Star III receiver, shown in figure 9, provides a qualitative measure of the signal attenuations during the test. Availability with the standard receiver varies rapidly between 0 and 11 satellites, due to foliage variations, while the high sensitivity receiver is able to track seven or more satellites at all times. Satellite visibility is higher in the latter case because of the enhanced signal tracking sensitivity which is the primary advantage of such a receiver under signal degraded conditions. Figure 10 shows the reference trajectory (smoothed solution from the tightly coupled OEM4/HG1700 integrated system). This reference trajectory is accurate to about 1 m.

Table 1. 2D position error distribution—LSQ GPS solution.

2D position thresholds (m)	<5	5–10	10–20	20+
(%)	74.1	21.7	3.0	1.2

GPS only results

This section quantifies the quality of the solution obtained from the SiRF Star III receiver. The results were obtained using the $C^3NAVG^2_{TM}$ software, developed by the PLAN Group of the University of Calgary (see footnote 1). $C^3NAVG^2_{TM}$ processes GPS pseudorange and Doppler measurements using a least-squares method (Petovello *et al* 2000). The use of an epoch-by-epoch least-squares solution is advantageous for analyzing the effects of measurement errors as no smoothing (as in the case of a Kalman filter) occurs. Figure 11 shows the trajectory obtained. As can be noted the solution is quite noisy and includes occasional jumps and spikes. These are caused by changes in the satellite geometry and large noise and multipath effects. Such effects are common under attenuated signal conditions. In a commercial system, these effects would be smoothed using an appropriate filter. Table 1 shows the position error distribution for the solution. Even though more than six satellites were visible throughout the test, 26% of epochs have errors greater than 5 m, indicating poor quality of the measurements. The reason for the poor measurement quality is the low C/N_0 of the signal received due to signal attenuation caused by the tree coverage and multipath. Figure 12 shows the carrier-to-noise density for all the satellites. As can be seen, during the initialization at the beginning when the user was in an open area, the signal power received is over 40 db Hz for all the satellites; however, during the actual walk under dense canopy the received signal power dropped by as much as 20 dB. Such a low-signal power increases the thermal noise jitter in the code tracking loops, leading to noisy measurements. The overall horizontal position RMS error is 5.3 m.

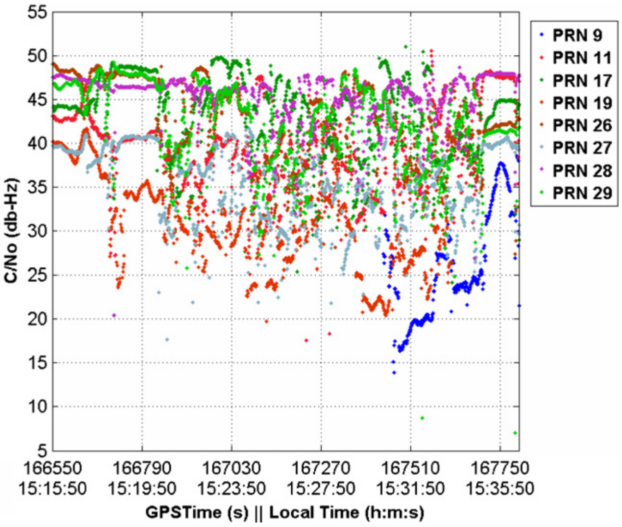

Figure 12. Carrier-to-noise density—SiRF Star III.

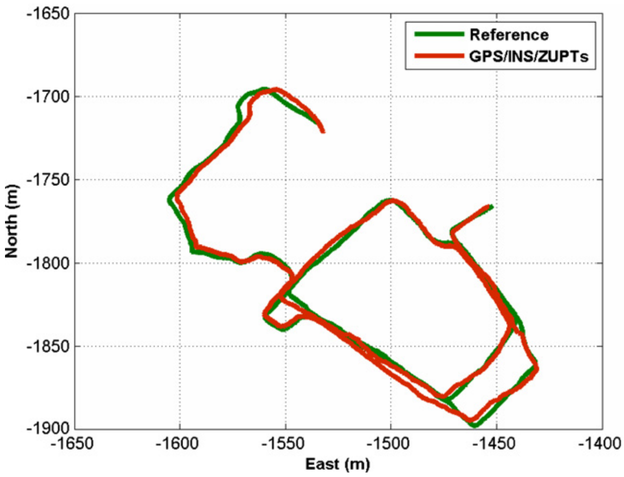

Figure 13. GPS/INS/ZUPTs integrated solution—Crista/SiRF.

GPS/INS/ZUPTs integrated results

Figure 13 shows the results obtained through the integration of the Crista IMU and SiRF Star III GPS receiver. The estimated trajectory is closely aligned with the reference trajectory. The INS was operating in the prediction mode using the GPS measurements available to control its errors, thereby keeping its accuracy bounded. The effect of the noise seen in the 'GPS only solution' is not visible in the integrated trajectory. This is because a Kalman filter is used for fusion of the two systems. The filter restricts the solution to certain limits determined by the predicted solution and the corresponding standard deviations and system noise, which ultimately introduce smoothing effects in the solution. An innovation-based reliability check method was also used to detect and reject the faulty GPS measurements. In a GPS/INS integrated system the predicted solution is derived from INS, which is fairly accurate given that the ZUPTs are used frequently to update the system. This ultimately enhances system capability to detect and reject faulty/noisy GPS measurements from the processing. Table 2 shows the position error distribution for this solution. The maximum horizontal error seen during the trajectory is 14 m, and the RMS error was 3.9 m. Availability was 100%.

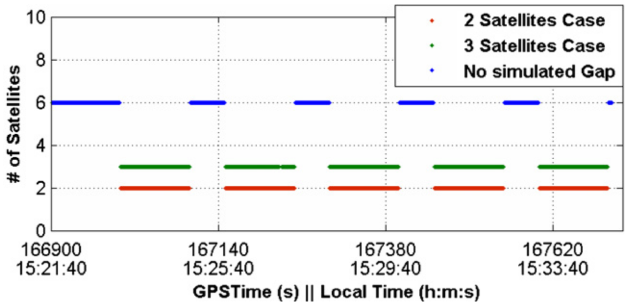

Figure 14. Satellite availability during gaps.

Table 2. 2D position error distribution—GPS/INS/ZUPTs solution.

2D position thresholds (m)	<5	5–10	10–20
(%)	86.5	9.4	4.1

Since more than six satellites were visible throughout the trajectory, the results do not fully demonstrate the prediction capability of the INS under poor GPS availability. To demonstrate this, partial GPS gaps were introduced at five different portions of the trajectory, each lasting 100 s. Two processing cases were considered. In the first case, three satellites were made available for the duration of the simulated gap, while in the second case, only two satellites were made available, as shown in figure 14. These gaps were simulated by rejecting the lowest elevation satellite from the processing as long as the number of satellites was greater than two or three. The results are compared to the case when no GPS gaps were simulated to obtain an assessment of actual errors caused by the INS predictions. Figures 15 and 16 show the trajectories obtained in each case and the places where gaps were simulated.

As can be noted, with three satellites available and with frequent ZUPTs, the INS predicted the navigation solution quite accurately during simulated gaps almost coinciding with the actual trajectory. To get a statistical assessment of the system performance the position errors were computed as a function of time since the last GPS update for each simulated outage. Using the resulting five error time series (i.e. one for every simulated outage), the RMS time series across all data gaps was computed, which is shown in figure 17. As can be noted the maximum error remained under 2.2 m for partial outage durations of 100 s.

Performance is poorer during the simulated gaps when only two satellites were made available, especially during the first gap. This is mainly because of an accumulation of heading errors. Although the distance propagated by the INS is quite accurate, heading errors cause significant position displacements. The maximum error seen after 100 s with only two satellites available is 5.5 m.

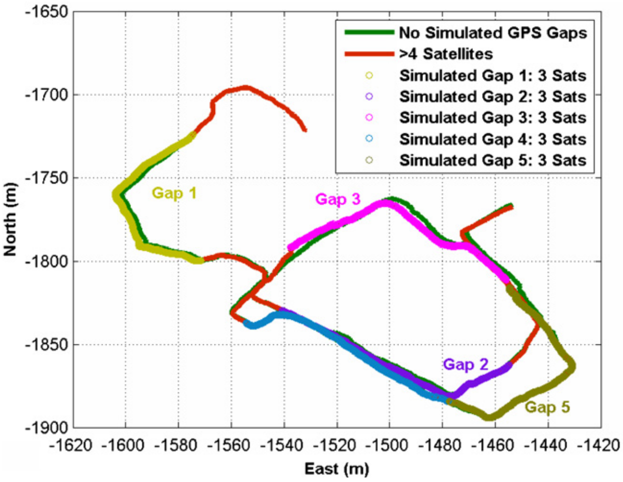

Figure 15. Trajectory with partial gaps—three satellites.

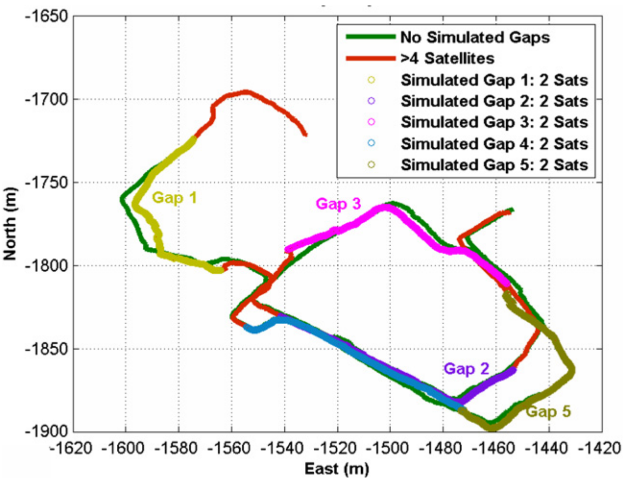

Figure 16. Trajectory with partial gaps—two satellites.

Conclusions and future work

This paper discussed the design of a low-cost foot-mounted pedestrian navigation system (PNS) based on a tight integration of a HSGPS receiver and a MEMS-based INS. The designed system takes advantage of the fact that the foot comes to rest every time it rests on the ground, and uses frequent ZUPTs measurements to keep the INS velocity and position errors bounded. The system performance was evaluated indoors with no GPS available and in forest areas under partial GPS outages. Overall the designed system performed quite well, and the results showed that the integrated system designed here can potentially be used for navigation in these challenging GPS environments. However, several further improvements and enhancements can be made. More specifically, external aiding sensors (such as a magnetometer) are required to keep the heading errors bounded, as these were identified as a primary performance limiting factor in the system.

Future research will focus on improving the accuracy of the heading estimate, through the use of external magnetometer sensors. The use of an external barometric sensor operating in a differential mode to eliminate atmospheric pressure variation will also be explored to strengthen the INS vertical component. The system's performance will be evaluated under different operating conditions, including dense urban and forest areas, using different conventional and high-sensitivity GPS receiver technologies.

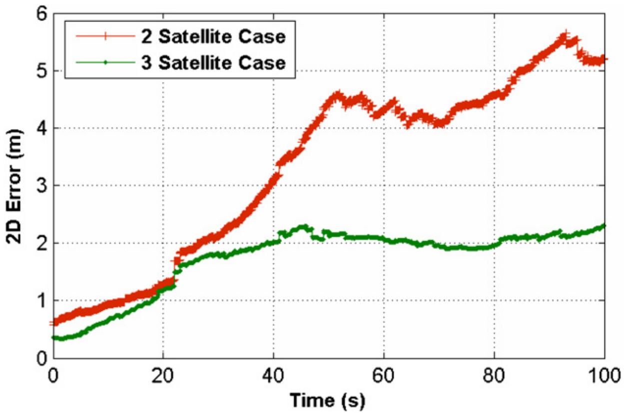

Figure 17. RMS horizontal errors of five outages.

Acknowledgments

The author would like to thank AUTO21 Networks of Centres of Excellence (NCE) and the Informatics Circle of Research Excellence (iCORE) for providing the financial support for this research.

References

Cao F X, Yang D K, Xu A G, Ma J, Xiao W D, Law C L, Ling K V and Chua H C 2002 Low cost SINS/GPS integration for land vehicle navigation *Proc. Int. Transp. Syst. IEEE* pp 910–3

Cavallo F, Sabatini A M and Genovese V 2005 Step toward GPS/INS personal navigation systems: real time assessment of gait by foot inertial sensing. intelligent robots and systems *IEEE/RSJ Int. Conf.* pp 1187–91

Chai H M 2004 *Applications of Kinesiology—Gait During Ambulation* (http://www.pt.ntu.edu.tw/hmchai/Kines04/KINoutline.htm)

Crista Interface/Operation Document 2004 *Crista Inertial Measurement Unit (IMU) Interface/Operation Document* A Cloud Cap Technology Inc.

El-Sheimy N 2004 Inertial Techniques and INS/DGPS Integration *ENGO 623-Course Notes* Department of Geomatics Engineering, University of Calgary, Canada

Farrell J A and Barth M 2001 *The Global Positioning System & Inertial Navigation* (New York: McGraw-Hill)

Godha S 2006 Performance evaluation of a low cost DGPS MEMS-based IMU integrated with DGPS for land vehicle navigation application *MSc Thesis* Department of Geomatics Engineering, University of Calgary, Canada, *UCGE Report No* 20239

Godha S, Lachapelle G and Cannon M E 2006 GPS/INS system for pedestrian navigation in a signal degraded environment *Proc. ION GNSS (US Institute of Navigation, Fort Worth, TX)*

Karunanayake D, Cannon M E, Lachapelle G and Cox G 2004 Evaluation of AGPS in weak signal environments using a hardware simulator *Proc. ION GPS/GNSS (US Institute of Navigation, Long Beach, CA, 21–24 Sept.)* pp 2416–26

Kealy A, Young S, Leahy F and Cross P 2001 Improving the performance of satellite navigation systems for land mobile applications through the integration of MEMS inertial sensors *Proc. ION GPS (US Institute of Navigation, Sept.)* pp 1394–402

Lachapelle G 2006 Pedestrian navigation with high sensitivity GPS receivers and MEMS *J. Personal Ubiquitous Comput.* Springer, published online, 10Oct06, (web http://dx.doi.org/10.1007/s00779-006-0094-3)

Lachapelle G, Mezentsev O, Collin J and MacGougan G 2003 Pedestrian and vehicular navigation under signal masking using integrated HSGPS and self contained sensor technologies *11th World Congress (Berlin: International Association of Institutes of Navigation)*

Ladetto Q 2000 On foot navigation: continuous step calibration using both complementary recursive prediction and adaptive Kalman filtering *Proc. ION GPS/GNSS (US Institute of Navigation, Salt Lake City, UT, 19–22 Sept.)* pp 1735–40

MacGougan G 2003 High sensitivity GPS performance analysis in degraded signal environments *MSc Thesis* Department of Geomatics Engineering, University of Calgary, Canada, *UCGE Report No.* 20176

MacGougan G, Lachapelle G, Klukas R, Siu K, Garin L, Shewfelt J and Cox G 2002 *Performance Analysis of A Stand-Alone High Sensitivity Receiver. GPS Solutions* vol 6 (Berlin: Springer) pp 179–95

Mezentsev O 2005 Sensor aiding of HSGPS pedestrian navigation *PhD Thesis* The University of Calgary, Department of Geomatics Engineering, Calgary

Mezentsev O, Lachapelle G and Collin J 2005 Pedestrian dead reckoning—a solution to navigation in GPS signal degraded areas *Geomatica* **59** 175–82

Petovello M, Cannon M E and Lachapelle G 2000 *C³NavG²™ Operating Manual* (Calgary: The University of Calgary, Department of Geomatics Engineering)

Salychev O S 1998 *Inertial Systems in Navigation and Geophysics* (Bauman: MSTU Press)

Savage P G 2000 *Strapdown Analytics* vol 1 (Maple Plain, MN: (Strapdown Associates))

Scherzinger B 2004 *Estimation with Application to Navigation* (ENGO 699.11-Course Notes) (Canada: Department of Geomatics Engineering, University of Calgary)

Stirling R, J Collin, K Fyfe and Lachapelle G 2003 An innovative shoe-mounted pedestrian navigation system *Proc. GNSS 2003 (Graz, Austria, 22–25 April)*